Energy and Technology Review

Lawrence Livermore National Laboratory

May 1988

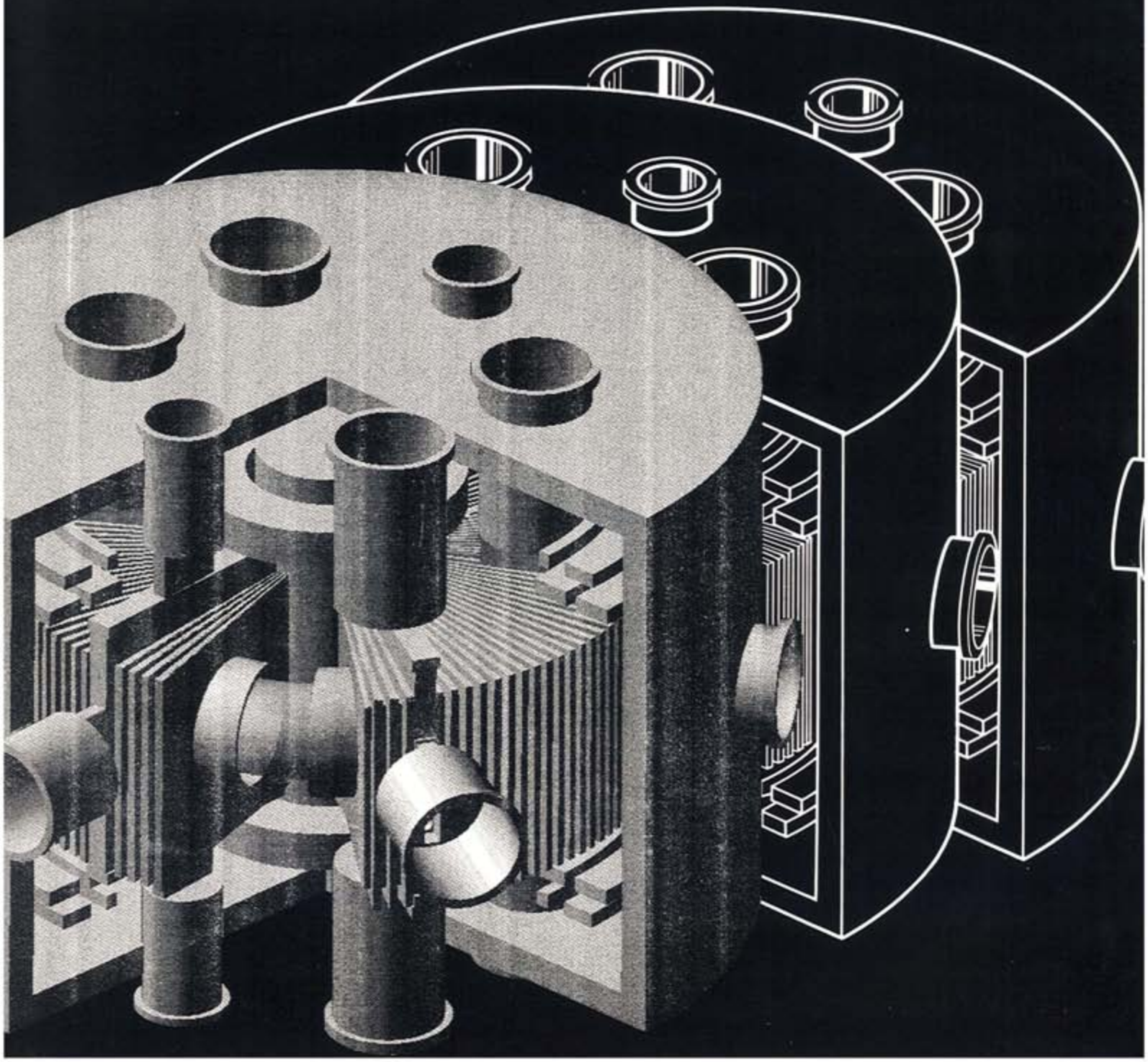

Gas Cooling of Laser Disks

Solid-state disk amplifiers can produce near-diffraction-limited, repetitively pulsed output beams if they are cooled on their surfaces by a heat-transfer medium of excellent optical quality. Our experiments and models show that effective cooling can be provided by flowing gas in adjacent channels across laser disk surfaces.

For further information contact Georg F. Albrecht (415) 423-7562 or Steven B. Sutton (415) 422-0322.

Since the earliest days of lasers, the scaling of solid-state lasers to significant average powers (i.e., relatively high pulse-repetition rates) while maintaining high beam quality has been considered a difficult problem. It was thought that waste heat, generated in the optical pumping process, could not be removed in such a manner as to reduce thermally induced optical distortions to an acceptable level. However, recent analysis[1,2] showed that this problem could be overcome by using a geometry in which thin disks are optically pumped and heat is removed from their large faces and across the thinnest dimension. This amplifier architecture is very similar to the Nova laser disk amplifiers developed for single-shot fusion experiments,[3] but with a cooling subsystem added.

The thrust of our present work is to assess quantitatively the performance potential of the flow-cooling disk concept by taking experimental measurements of optical beam quality over a wide range of cooling parameters and by developing and validating quantitative design codes. Our work to date supports the conclusion that we can design adequately cooled solid-state laser amplifiers approaching a megawatt of high-quality output power per square meter of aperture.

The active medium in a solid-state laser disk amplifier is a thin, rectangular plate or slab with side lengths in a ratio of about 2:1. This plate is oriented with respect to the output beam direction at an angle that minimizes reflection losses (i.e., Brewster's angle). To effectively cool such a plate, heat must be removed from the largest surface across the thinnest dimension. Since the laser beam traverses the slab through its large faces, the cooling medium that draws heat from the slab must have excellent optical quality and must be unaffected by the heat-removal process. These considerations lead to the choice of a gas as the coolant.

Accordingly, we have investigated the flow of a gas over a hot surface in a confined flow channel (Figure 1). We must understand not only the bulk flow properties and their effect on eventual optical distortions of the slab and the separation windows but also the optical properties of the gas flow itself. We have therefore undertaken an experimental and modeling effort to examine in detail

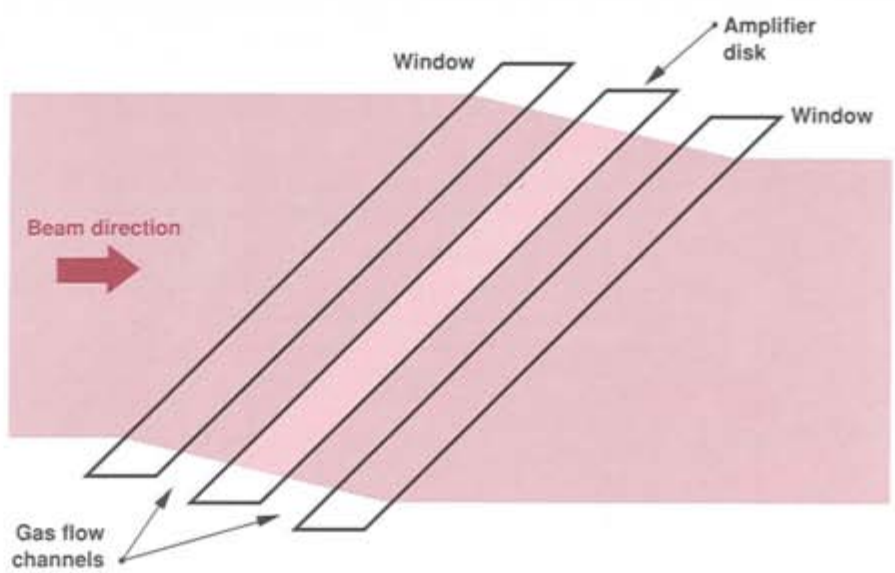

Figure 1. A cross section of the geometry of an amplifier disk, the cooling gas, and the laser beam in a gas-cooled disk amplifier.

the fluid dynamics, heat transfer, and optical properties of a section of channel flow.

Cooling Channel Geometry

Typical channel geometry is shown in Figure 2. Cooling effectiveness in the channels can be characterized by parameters that affect laser system performance (e.g., slab temperature and temperature gradient along the slab). Each of these parameters is dependent on a number of flow and fluid parameters, such as Mach number, pressure, and the flow geometry. For example, Figure 3 depicts the effect of flow Mach number and pressure on the temperature drop in the thermal boundary layer. At first glance, it appears that two ways to reduce the slab temperature are to increase the Mach number or increase the gas pressure. However, frictional drag (which consumes compressor power) increases with pressure and with the cube of the Mach number; increased pressure also increases the distortion of optical components in the system. To maintain a high overall system efficiency, we wish to use the minimum amount of compressor power needed to achieve the desired degree of cooling that is consistent with acceptable optical distortions. Thus, proper cooling of the laser slab requires the correct choice of flow geometry, gas type, and flow conditions to extract the heat at tolerable levels of compressor power and optical distortion.

Flow Design

Flow design begins with the nozzle. A properly designed nozzle efficiently exchanges internal energy for kinetic energy (pressure for flow) while introducing little disturbance into the flow stream. The nozzle takes low-velocity gas provided by the driving compressor and accelerates it with a significant reduction in the static pressure and temperature of the gas but with negligible reduction in the stagnation pressure and temperature. Flow exiting the nozzle has a high velocity, which is required for efficient cooling, and a nearly uniform velocity profile.

As the flow travels down the narrow channel, the presence of the walls causes the formation of viscous boundary layers. A boundary layer is a zone of accommodation between regions of different flow characteristics. In a viscous boundary layer, the transition is between a high-velocity core flow and the zero-velocity flow at the channel walls. At the channel entrance, where the viscous influence zone is thinnest, frictional forces are at their largest. As the flow develops (see Figure 4), the viscous boundary layer grows and the velocity gradient and shear stresses at the wall decrease. The viscous development continues until the wall effects and the velocity profile have stabilized. The retardation of flow is accompanied by a decrease in both the static and stagnation pressures.

Gas Temperature, Velocity, and Density

Now let us consider gas temperature. In the configuration shown in Figure 4, the walls upstream of the slab are adiabatic (no heat transfer). In this region, shear-generated energy causes a slight warming of the gas wherever there

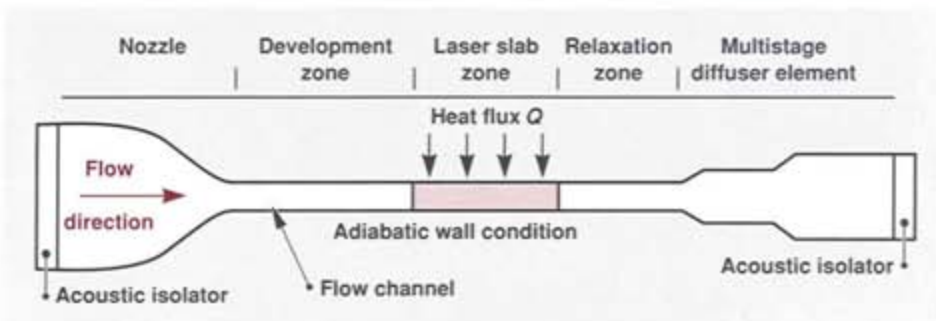

Figure 2. A schematic representation of a cooling channel, showing typical channel geometry. An inlet nozzle takes high-pressure, low-velocity gas from the system compressor and injects it into the flow channel. The cooling gas is conditioned both hydrodynamically and thermally in the development portion of the flow channel. The intermediate region of the channel encompasses the laser slab, where heat is removed by the fluid. Beyond the laser slab (downstream) is a relaxation region, followed by a diffuser element where kinetic energy is recovered from the flow.

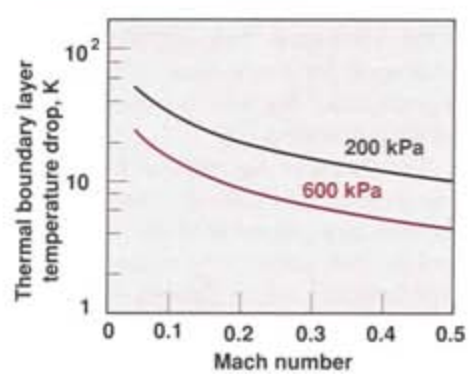

Figure 3. The effect of Mach number and pressure on the convective heat transfer temperature drop in a 4.5-mm channel with a surface heat flux of 2 W/cm^2.

exists a strong velocity gradient. In the slab region, in order to remove heat, the surface temperature must be greater than the gas temperature. As with the velocity, this temperature difference results in the formation of a thermal boundary layer with steep temperature gradients in the gas near the surface. The temperature gradients allow energy to "diffuse," again primarily through turbulent action, through the boundary layer and out into the core flow, thus increasing the thickness of the thermal boundary layer. Like the viscous boundary layer, this thermal boundary layer grows across the channel until something resembling a fully developed profile is achieved. Note that the viscous profile is symmetric whereas the thermal profile is asymmetric, because heat is being removed from only one side of the channel.

Since we use a gas for cooling, changes in temperature and pressure strongly affect the gas density. Figure 4 includes the density profile through the channel, which is seen to vary inversely with the temperature. Any variation down the channel of either the cross-stream density gradients or the bulk density can introduce aberrations into the extraction beam.

The high-velocity gas decelerates in the diffuser before it is returned to the compressor, converting some kinetic energy to internal energy. This causes an increase in both the static temperature and pressure. Diffusers are not as efficient as nozzles. It is difficult to transfer more than about 70% of the available kinetic energy back into internal energy.

The frictional losses in the cooling channel and the recovery losses in the diffuser contribute to the pressure difference necessary to

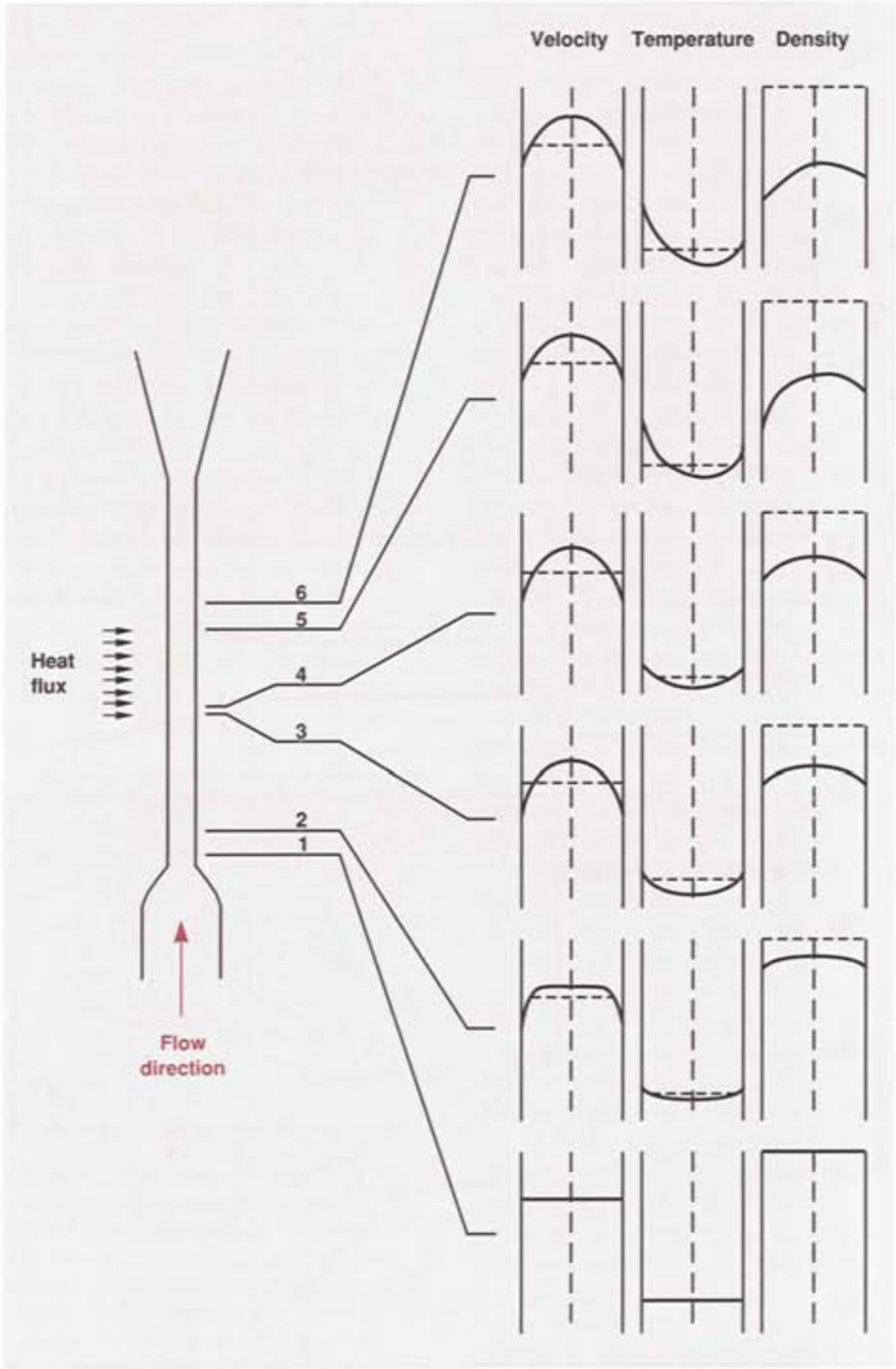

Figure 4. Diagram of flow development in the cooling channel.

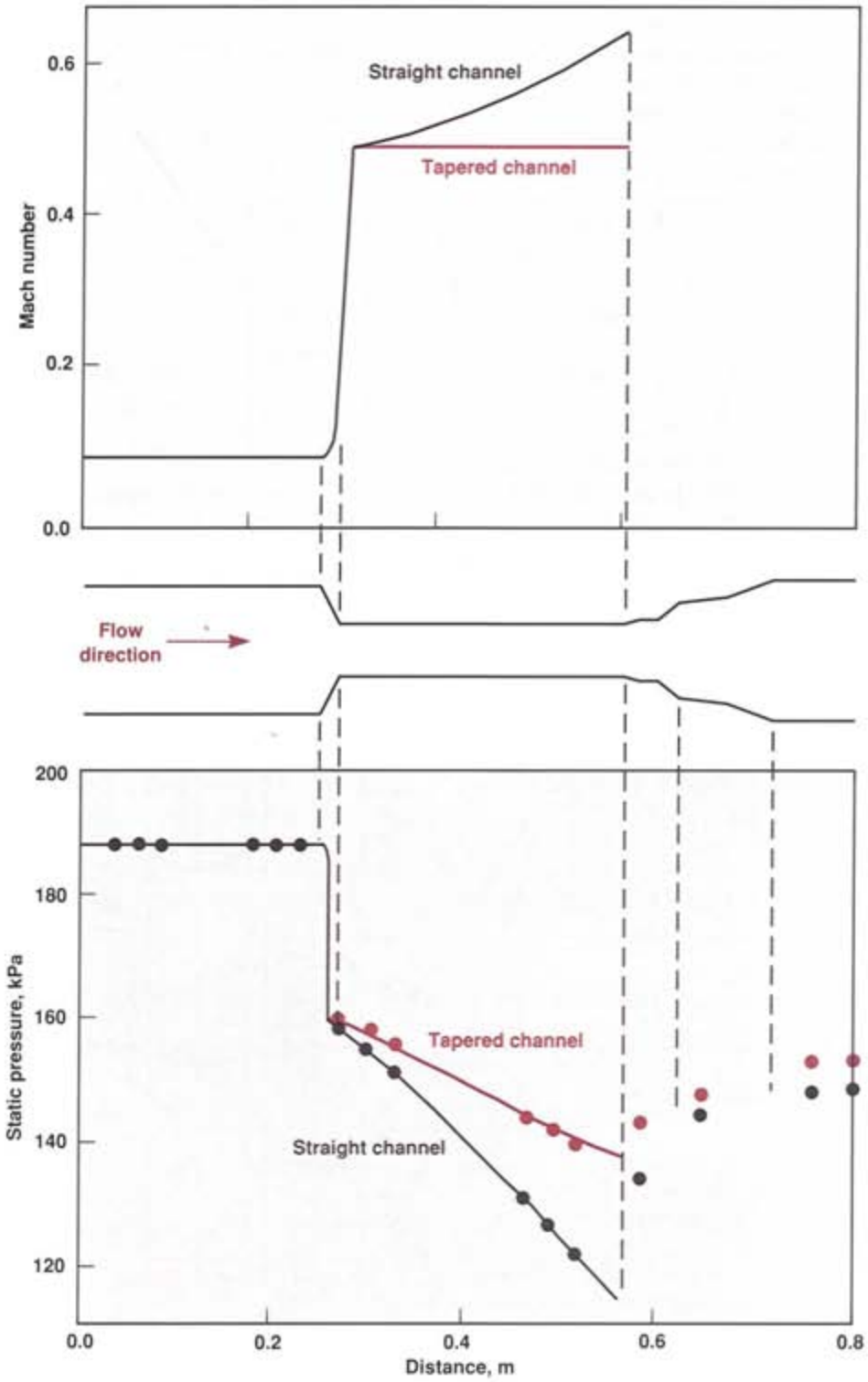

Figure 5. Calculated Mach numbers and a comparison of calculated (curves) and measured (data points) static pressures in a straight and a tapered (0.05-deg) channel.

drive the flow through the cooling loop. Since the compressor power is directly related to the overall stagnation pressure drop, we must design the least lossy, most thermally efficient cooling arrangement possible. The compressor power and thermal conditioning power represent sacrifices in the single-shot efficiency that must be made in order to operate the laser at average power.

To optimize the cooling system, we must understand gas flow and heat transfer from a system viewpoint. We must also understand the effect of heat transfer and flow behavior on optical distortions in the laser materials. To do this, we used three types of models:

(1) Analytical solutions to the one-dimensional flow equations for the special flow conditions of constant area with friction (Fanno flow) and variable area with constant Mach number, friction, and heat addition (a tapered channel).

(2) Numerical integration of the general one-dimensional flow equations that include the effects of area change, friction, and heating, using experimental correlations for boundary effects.

(3) Numerical integration of the two-dimensional Navier-Stokes equations using high-order turbulence modeling. For this, we employed the TEXSTAN computer program[4] that integrates the steady, compressible, boundary-layer form of the Navier-Stokes equations for mass, momentum, and energy.

Experiments

We performed many extensively instrumented experiments to collect information on the bulk character of the channel flow and to gather data for validating the various numerical approaches. In all cases, we used nitrogen as the cooling fluid.

Pressure

We measured the static pressures in the channel, since they are associated with flow-separation window pressure distortion. We also concentrated on the surface temperature and the gas temperature, since they influence thermal distortion of the slab and flow separation window, which in turn creates optical distortions.

We measured static pressures upstream, downstream, and along the channel with 16 static pressure taps and a pressure gauge. Figure 5 compares the measured and predicted static pressure for a constant-area channel and a tapered channel (0.05-deg taper). The associated flow Mach numbers are also shown. Good agreement between measured and calculated static pressures is achieved through the nozzle and the channel. However, the models are not sophisticated enough to model the diffuser flow. Figure 5 clearly shows both the effect of the nozzle in increasing the velocity and reducing the static pressure, and the effect of the diffuser in recovering some of the nozzle pressure drop. Figure 5 also shows the effect of a very slight channel taper on reducing the static pressure drop at moderate Mach numbers, thus offering a geometry variation that can be used to reduce pressure imbalance distortions in the optical components.

Temperature

There are two issues that must be considered with respect to temperature: (1) the magnitude of the surface temperature, which is a measure of the slab temperature and influences lasing gain and optical distortions, and (2) the thermal profiles of the boundary layer, which pertain to scattering losses within the cooling gas. We have simulated thermal load with an electrically heated indium/tin-oxide resistive coating at the slab location. We measured gas temperature within the thermal boundary layer with a small thermistor mounted to a hot-wire probe support. The surface temperature was measured using thermal imagery.

Figure 6 compares probe temperatures as calculated by the TEXSTAN code and as measured by an intrusive thermal probe for flow in a 3-mm-thick straight channel. In interpreting the measured temperature, it is important to note that flow stagnates at the leading edge of any blunt object. Thus the thermal probe does not necessarily see the static temperature of the gas but rather a temperature more closely associated with stagnation conditions. Thermal conduction within the gas reduces the measured temperature somewhat below the stagnation temperature. The additional lines on the ordinates of Figure 6 give values for the calculated and measured surface temperatures. The calculations capture very well both the shape and magnitude of the gas temperature. Figure 6 also shows the very steep temperature gradients that occur in the vicinity of the wall.

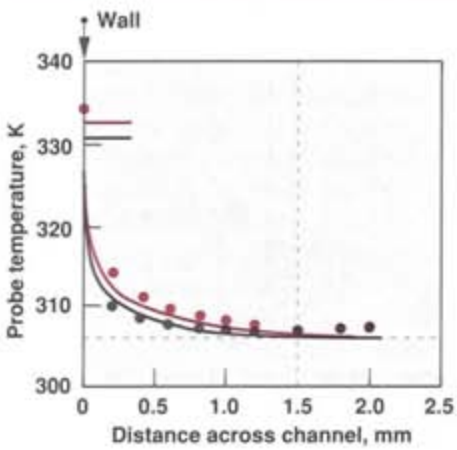

Figure 6. Comparison of measured and calculated probe temperatures in a Mach-0.4 flow with a surface heat flux of 1.67 W/cm^2. Upstream temperatures are shown in black; downstream temperatures in color; data points denote measured temperatures; curves denote calculated temperatures. The additional black and colored lines and data point near 330 K on the ordinate give values for the calculated and measured surface temperatures.

The TEXSTAN-calculated slab-surface temperature profile reveals the importance of properly considering thermal boundary layer development. It is only after a relatively long development length that the TEXSTAN-calculated surface-temperature gradient approaches the value associated with simple caloric heating. This has caused us to consider thermally preconditioning the flow upstream of the slab, using resistive heating, to minimize the cooling variations along the active medium.

So far, we have explored bulk flow properties of compressible channel flow as they relate to pressure and temperature profiles. These profiles determine how much surface heat flux can reasonably be removed and indicate the resulting deformations in the slab and the channel separation windows, which in turn determine some of the beam aberrations in the laser system. In general, our results show the predictive accuracy of our numerical approaches and their usefulness as tools for designing future experiments and for exploring optimized configurations that we cannot investigate experimentally.

Optical Properties of the Gas Flow

In a generic disk amplifier architecture, the beam must traverse two types of gas flow. The first is channel flow, whose bulk properties we discussed above. The second type of flow occurs in the regions between the disks, which we call the drift region (see Figure 7). It is not desirable to simply trap gas in the drift region, since thermal convection within these long-optical-path-length regions would give rise to severe beam distortions. Therefore, the flow in the drift region must be conditioned to moderate thermal convection currents and temperature gradients in the gas.

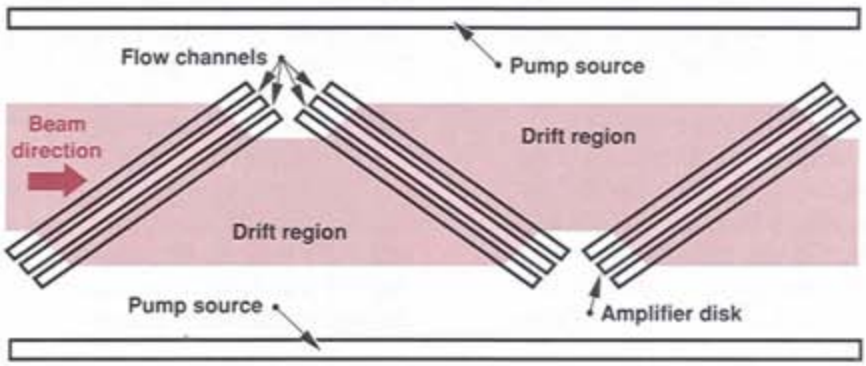

Figure 7. The drift region is the space between amplifier disks. The flow there must be conditioned to minimize beam distortions.

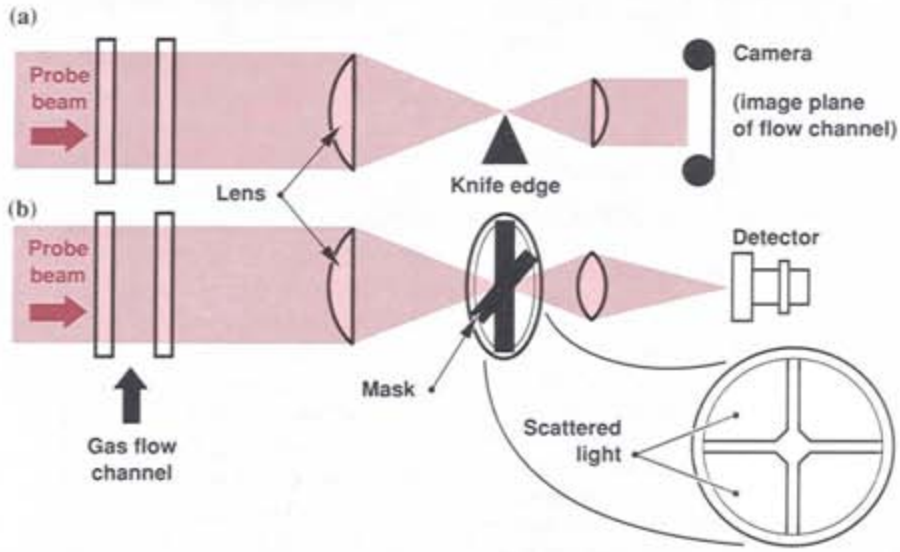

Figure 8. A Schlieren setup visualizes refractive index gradients by passing only deflected rays past the knife edge (a). If the scattered light is collected in a detector (b), the amount can be measured.

Turbulent Scattering. Turbulent scattering, like all scattering, arises from variations in the index of refraction in the medium traversed by the beam.[5] Since the index of refraction of a gas depends on its density (which in turn depends on temperature and pressure), fluctuations in the pressure and temperature cause scattering.

Pressure fluctuations arise mainly from local turbulent velocity fluctuations and acoustic waves propagating through the gas. The acoustic waves are related to boundary layer instabilities, like the trend toward transitory velocity stall at the diffuser walls.

Temperature fluctuations in the flow channel arise from the boundary layer at the heated slab. Since turbulence generation consists, so to speak, of the removal of a small parcel of sublayer fluid through a shear-driven instability, a piece of very hot gas from near the wall is carried out into midstream, where it is registered by a probe beam as a temperature fluctuation.

In the drift region the same basic process occurs. Possible large-scale temperature gradients across the reflector plate must be averaged out quickly or we will have much the same large-scale temperature problem as we encountered with convective recirculation. To accomplish this, we have the gas leave the reflector plate through an array of small holes or jets. The many jets generate a background of high turbulent intensity that rapidly mixes the drift region gas and breaks up the large-scale temperature gradients into small-scale local temperature fluctuations.

Schlieren Experiments. To investigate experimentally the problem of light scattering by a

turbulent flow, we used the Schlieren method (Figure 8), commonly used to look at refractive index variations. The collimated beam from a laser is directed through the flow channel or the drift region. Most of the light rays pass undisturbed through the region in question, and are imaged by a lens to form a far-field diffraction pattern that corresponds to the aperture that the test object presents to the beam. Some of the rays, however, are deflected.

If we place an obstacle, like a knife edge, at the focus, we can stop the undeflected rays from propagating further and only the deflected rays travel past the knife edge. The deflected light can then be used to form an image of the flow channel or drift region. This image maps the locations in the aperture where the ray deflection took place, thus indicating how uniformly scatterers are distributed across the aperture. Since the pulse from the laser is much shorter than the time it takes the gas to flow across the aperture, the laser pulse freezes the motion of the gas in the channel. Finally, as indicated in Figure 8, we can collect all the scattered light in a photodetector and determine the ratio of the deflected light to the intensity incident from the laser. In this way, quantitative measurements of the scattered intensity can be made. Below, we give a few examples of such measurements as they were made with the flow channel and the drift region.

(a) No flow

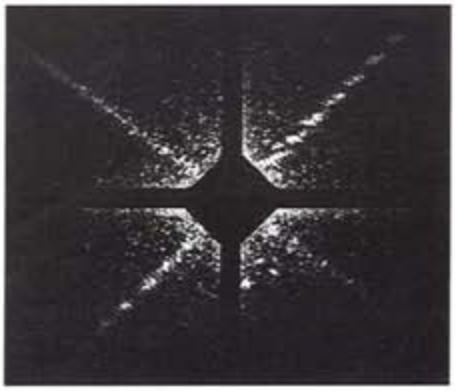

(b) Flow (Mach 0.6)

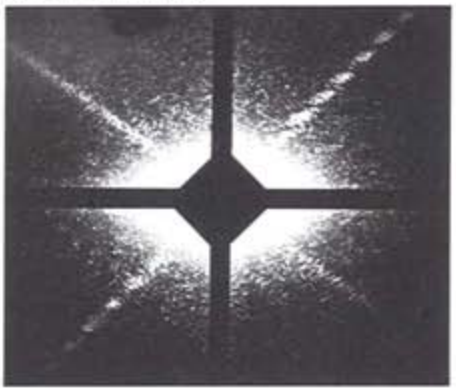

Figure 9. Intensity distribution in the focal plane with the flow channel as the test object. The halo of scattered light around the mask covering the diffraction pattern is clearly visible. Its shape and size allow us to draw conclusions about the shape and size of the turbulent features in the flow channel.

Figure 9 shows the focal plane of the lens that collects the scattered light. We used a cross mask (instead of a knife edge) to block out the cross-shaped diffraction pattern arising from the square aperture that the flow channel window presents to the probe beam. Around the mask we clearly see the elliptical halo of light that was scattered by the turbulent flow features in the channel. Several quantities of interest can be deduced from this picture. First, the light is typically scattered into an elliptical cone of 1.3×0.75 mrad, which corresponds to an average size of the scatterers in the flow channel of 1.5×0.8 mm. Hence we can say that the average eddy that causes the scattering is elliptical in shape, with the long direction aligned with the flow and, at 0.8 mm, has a thickness of about one-quarter of that of the flow channel. If we form an image of the flow channel with the scattered light, we obtain the picture in Figure 10a. This shows that the scatterers are uniformly distributed across the aperture and scattering levels are so low that optical imperfections become clearly visible. Figure 10b is a picture obtained with a different nozzle, where the distribution of scatterers, and thus the

(a) Mach 0.64 Flow direction

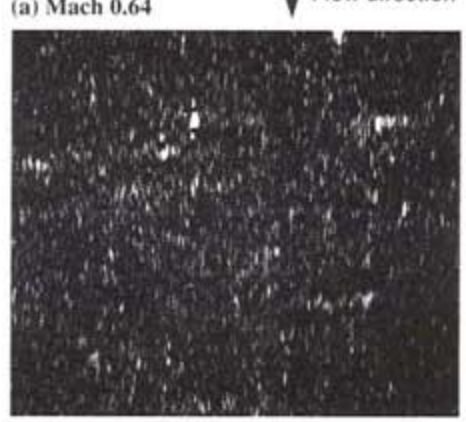

(b) Mach 0.3

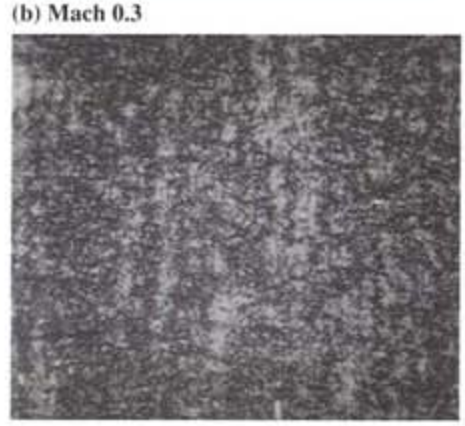

Figure 10. Schlieren pictures of two flow channels. (a) A 3-mm-wide flow channel at Mach 0.64. The flow is well conditioned, the distribution of scatterers across the aperture is uniform, and overall scattering levels are low. (b) A 5-mm-wide flow channel at Mach 0.3. The long features extending from top to bottom are most likely vortices generated by faulty nozzle design and not controlled by a sufficient flow development length. The distribution of scatterers is nonuniform and overall scattering levels are high.

heat transfer properties of the gas, is no longer uniform across the aperture.

Proportion of Light Scattered. We also determined the proportion of light scattered as a function of Mach number and channel width. The results (Figure 11) show that the scattered intensity scales as the Mach number to the fourth power. This strong dependence derives from a dependence of the scattered intensity on the square of density fluctuation, which in turn depends on the square of the Mach number. If we draw a vertical line through the plot at fixed Mach number, we find the scaling of scattered intensity with channel width. A good fit to the data is achieved by scaling the scattered intensity with the channel width to the 1.4th power. If the scatterers were all much smaller than the channel width, then, for small losses, one would expect a scaling that is linear with channel width. Deviations from this linear relation arise from the largest turbulence features in the flow, which have a dimension comparable to the channel width. (We should mention here that if one measures the scattering loss with an entirely different technique, one obtains a scaling law that is more closely proportional to the channel width. We are therefore inclined to look at the 1.4th power scaling as the upper limit.)

Effect of Thermal Boundary Layer. Refractive index fluctuations associated with pressure and temperature fluctuations within the thermal boundary layer produce turbulent scattering. Hence, one would expect the amount of light scattered to depend on the amount of surface heat flux pulled from the slab. Figure 12 quantifies this effect. It is clear that a slower flow (i.e., Mach 0.3 vs Mach 0.5) permits a hotter boundary layer, which means larger temperature fluctuations, which in turn means a larger thermal contribution to turbulent scattering of the probe beam.

The same methods described above for diagnosing turbulent scattering in the flow channel can be used on the drift region. The average flow velocity in the drift region is at most a few meters per second, corresponding to Mach numbers below 0.01; thus, scattering fluctuations from this source should be negligible. Turbulent scattering in the drift region depends essentially on temperature fluctuations only. These will arise, as mentioned above, from temperature gradients across the reflector plates through which the jets enter into the drift region.

In our experiment, we generated such a temperature difference by heating the center of the reflector plate and then measuring the temperature difference between

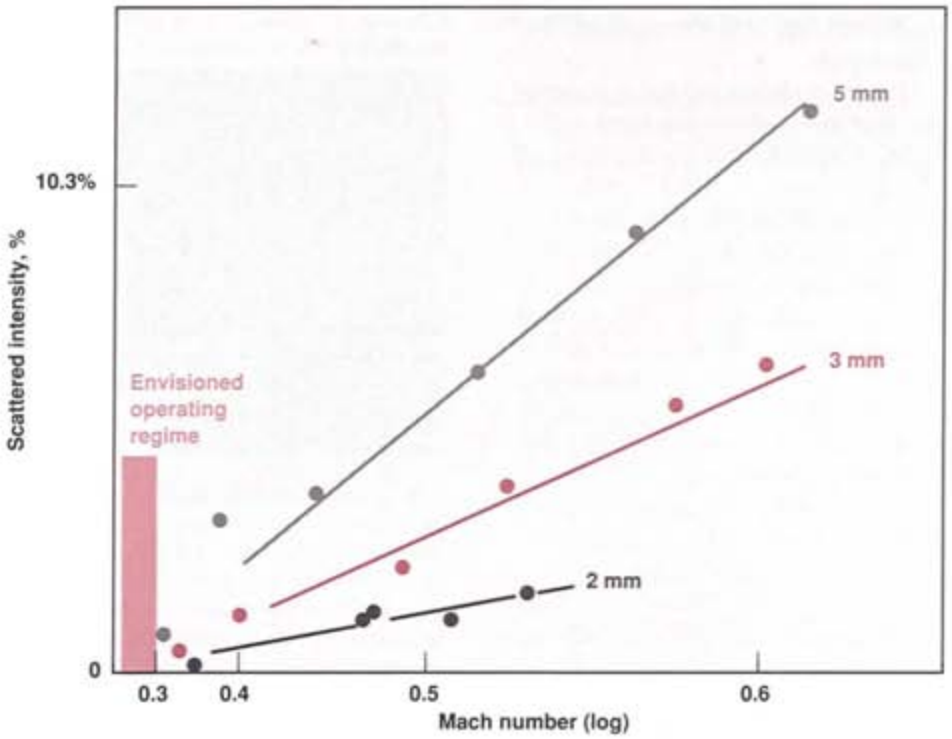

Figure 11. The scattered intensity as a function of the Mach number of the flow, measured for three different channel widths (2, 3, and 5 mm) with the modified Schlieren setup of Figure 8b. The scattering scales as the fourth power of the Mach number and the 1.4th power of the channel width.

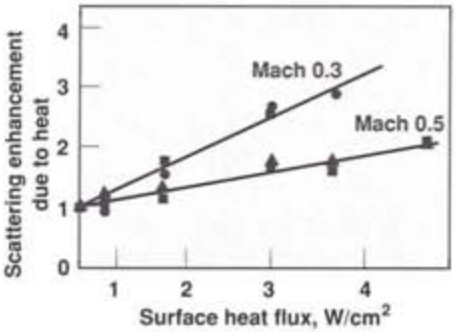

Figure 12. Enhancement factor of turbulent scattering due to passage of the gas over a hot surface. In a slower flow, the gas is heated to higher temperatures, which increases the magnitude of the temperature fluctuations and in turn increases the turbulent scattering.

center and edge. Since one would expect larger turbulent features at the lower flow rates prevalent in the drift region, we used a version of the setup in Figure 8 in which the probe beams makes a double pass through the drift region. This doubles the scattering angles and makes the halo of scattered light in the focus easier to observe. Figure 13 shows the focal plane for the Schlieren setup when the drift region is examined. The halo of scattered light is now circular and covers a much narrower cone. This means that the average turbulent feature size in the drift region is around 1–2 cm, which compares well with the spacing of the jets as they leave the reflector plate.

Figure 14 shows the approximate scattered intensity in the drift region as a function of center-to-edge temperature difference of the reflector plate through which the jets enter the drift region. As expected, the scattering is essentially independent of flow speed and depends on the temperature gradient only. It is equally clear that large-scale temperature gradients across the reflector plate must be avoided. For a given illumination nonuniformity, this can be achieved by water cooling the reflector from the back, which, for operation at significant average power, has to be done anyway.

Our turbulent scattering measurements so far have given us a good idea of the magnitude of the scattering, some of its most important scaling, and the origin and suppression of some undesirable flow instabilities. We have also found that under the conditions at which we eventually intend to operate an actual amplifier, the loss due to turbulent scattering can be held within very acceptable limits, particularly when helium is used instead of nitrogen. Our present efforts in this area are

(a) No flow

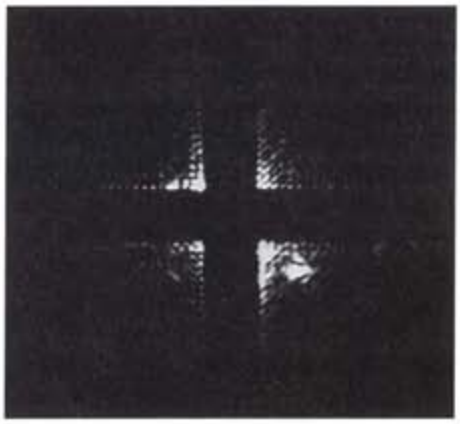

(b) Fast flow; no temperature gradient

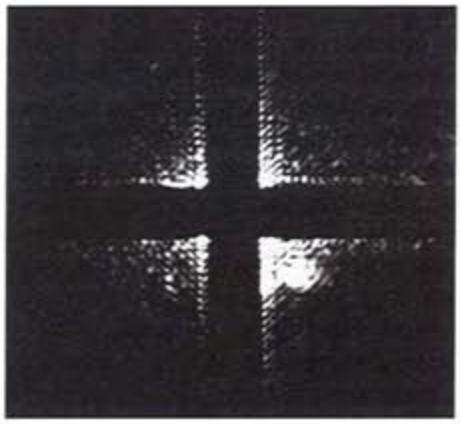

(c) Slow flow; temperature gradient

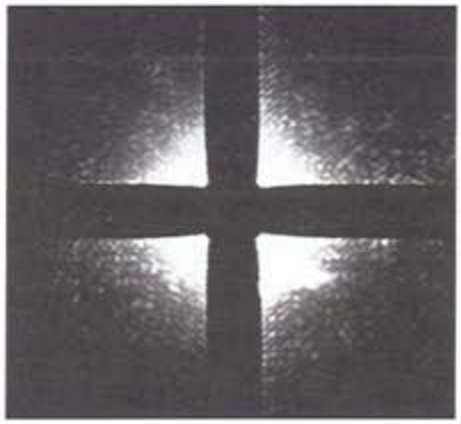

Figure 13. Intensity distribution in the focal plane with the drift region as the test object for (a) no flow, (b) flow at 1700 liters/min and no temperature gradient, and (c) flow at 850 liters/min and a temperature gradient of 17 K. The scattering occurs into much smaller angles and the average turbulent feature is not distorted into an ellipse. (Compare this figure with Figure 9 for the flow channel.)

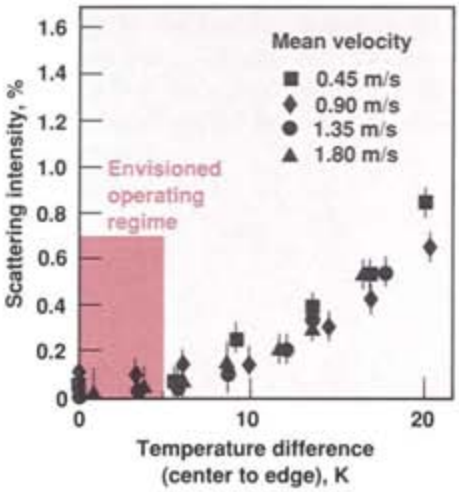

Figure 14. Scattered intensity as a function of center-to-edge temperature difference for different flow rates. The scattering is independent of flow rate. At the very low Mach numbers involved (around 0.003), this is to be expected.

directed at an increased understanding of the turbulence-generating mechanism in the drift region so that we can eventually achieve the required turbulent intensity with a well-understood minimum in compressor power requirements.

Conclusions

From our work to date, we are confident that we can design adequately cooled solid-state laser amplifiers approaching a megawatt of high-quality output power per square meter of aperture. With this ability to scale to such output powers while preserving beam quality plus the encouraging developments of diode laser pumping, the solid-state laser is truly technically competitive with respect to average power for very high-power applications, such as a laser driver for a fusion reactor.

Key Words: computer code—TEXSTAN; gas cooling; gas flow—turbulent; laser—disk amplifier, solid state.

Notes and References

1. J. L. Emmett, W. F. Krupke, and J. B. Trenholme, "The Future Development of High-Power Solid-State Lasers," *Soviet J. Quantum Electron.* **13,** 1 (1983).
2. J. L. Emmett, W. F. Krupke, and W. R. Sooy, *The Potential of High-Average-Power Solid-State Lasers*, Lawrence Livermore National Laboratory, Rept. UCRL-53571 (1984).
3. Disk amplifier development is described in the LLNL *Laser Program Annual Reports* from 1974 on.
4. TEXSTAN is a variation, produced by M. E. Crawford, of the STAN5 computer program: M. E. Crawford and W. M. Kays, STAN5—*A Program for Numerical Computation of Two-Dimensional Internal and External Boundary Layer Flows*, National Aeronautics and Space Administration, Rept. NASA CR-2742 (November 1976).
5. See for example, V. I. Tatarski, "The Effects of the Turbulent Atmosphere Wave Propagation," available from DoC, NTIS. ISBN-0-7065-0680-4. Translated from Russian in 1971.